1 Experimental Section

1.1 Materials

Commercial multi-walled CNTs (above 95% purity) with the diameter of 20–40nm and the length of 1–2 μm were obtained from Shenzhen Nanotech. Port. Co. Ltd. All Chemicals such as $H_2PtCl_6 \cdot 6H_2O$(≥37.5% Pt basis), $PdCl_2$(60% Pd basis), methanol (≥99.8%), ethanol (≥99.8%), 1-propyl alcohol (≥99.7%), D-glucose (≥99.5%), D_2O (≥99.9 atom % D), $NaHCO_3$ (≥99.5%), Na_2CO_3 (≥99.0%), $KHCO_3$ (≥99.0%), K_2CO_3 (≥99.0%), KOH (≥90.0%) and other carbonates in this paper were also purchased from Sigma-Aldrich and used as received. All the reagents used for the experiments were of analytical grade.

1.2 Catalysts preparation

Pt-Pd supported catalysts were prepared by wet step-impregnation and co-impregnation of CNTs with well-mixed $H_2PtCl_6 \cdot 6H_2O$ and $PdCl_2$ aqueous solutions. In co-impregnation method, the precursors were dissolved in deionized water according to the specified weight ratio of Pt:Pd (0-5 wt%:0-5wt%). The resultant solution and the support were mixed for 12 h, subjected to evacuation at 50 °C for 4 h. Finally, the sample was dried at 100 °C for 12 h, and calcined under Ar (40 mL min^{-1}) atmosphere at 400 °C for 2 h (heating rate 5 °C min^{-1}). After being cooled to room temperature, and reduced under H_2/Ar (20/40 mL min^{-1}) atmosphere at 300 °C for 2 h (heating rate 5 °C min^{-1}). Pt-Pd catalysts were denoted as Pt_xPd_y/CNTs, where x or y = 0,1,2,3,4 or 5 wt% are the theoretical loading. In the stepwise impregnation method, the impregnated support with the first precursor is dried and calcined and the thus obtained catalyst is mixed with aqueous solution of the second precursor and then dried and calcined as mentioned previously. In the synthesis procedure, if first Pt and then Pd precursors are impregnated on CNTs support consecutively, the sample is denoted as Pt/Pd/CNTs. If the order of impregnation is reversed the sample is denoted as Pd/Pt/CNTs.

1.3 Catalytic reaction procedure

Catalytic reactions were performed under anaerobic conditions in 50 mL, three-necked, round-bottom flasks. Before the addition of the catalyst and commencement of magnetic stirring, the solvent used in the reaction was carefully bubbled with Ar for 4 h under ultrasound. A similar experimental procedure was followed for contrast experiment. In a typical catalytic reaction, Pt_xPd_y/CNTs catalyst (0.1 g) was introduced into a glucose solution (0.06 mol mL^{-1} glucose in a solvent consisting 20 mL ethanol and 20 mL H_2O) with CO_2 source (0.16g K_2CO_3) at 30 °C. To assess the stability of the catalysts, it was used in successive catalytic cycles. After each cycle, the catalyst was recovered through filtration, washed with distilled water, before it was reused in the transfer hydrogenation of a freshly prepared solution of glucose and K_2CO_3.

1.4 Catalyst characterization

The Pt content was determined by inductively coupled plasmaoptical emission spectroscopy (ICP-OES). The samples were treated with perchloric acid and nitric acid solution, and the solution was filtered and analyzed by ICP-OES.

The samples were analyzed by transmission electron microscopy (TEM) (Philips CM200, 200 kV). HAADF-STEM and corresponding Elemental Mapping uses DX4 analysis system (EDAX) for analysis. Powder samples were ultrasonicated in ethanol and dispersed on copper grids covered with a porous carbon film.

The X-ray diffraction (XRD; Rigaku D/MAX-RB) patterns of samples were recorded at 100 mA and 40 kV in the 2θ range of 5–90° using monochromatised Cu K_α radiation and a scan rate of 10° min^{-1}.

The temperature-programmed reduction (TPR) of catalysts was conducted using a chemisorption analyser (AutoChemII2920). Prior to assessment, the catalyst (∼50 mg) was dehydrated in the isothermal region of a quartz U-tube reactor at 400 °C for 2 h in a flow of He (30 mL min^{-1}) to eliminate physisorbed water. Then, the catalyst was cooled to room temperature, and TPR curves were recorded in a flow of 10% H_2/He (30 mL min^{-1}) as the temperature was linearly increased to 700 °C at a heating rate of 5 °C min^{-1}.

Temperature -programmed desorption (H_2-TPD) of samples were achieved on a Quantachrome Chembet 3000 analyzer equipped with a TCD detector. In H_2-TPR, the tested sample was pretreated in argon atmosphere at 300 °C for 1 h and subsequently reduced from 50 to 300 °C with a heating ramp of 10 °C/min in 10 % H_2/Ar atmosphere. In H_2-TPD, 100 mg of sample was purged in the adsorbed gas (10 % H_2/Ar) at 50 °C for 30 min. Then, the sample was flashed with Ar to remove the physically adsorbed gas molecules, followed by heating at a rate of 10 °C/min in Ar from 50 to 700 °C, and the signals were recorded.

Fourier transform infrared attenuated total reflection spectra (ATR-FTIR), using a Thermo Fisher iN10 spectrometer equipped with a liquid-nitrogen-cooled MCT detector, were recorded within the spectral range of 650–4000 cm^{-1} with a resolution of 4 cm^{-1} and 16 scans for signal accumulation.

The spectroscopy of X-ray photoelectron (XPS) was executed employing a photoelectron spectrometer supplemented with a monochromatic source of Al KαX-ray, exerted at 20 mA and 15 kV. The reduction of catalysts was carried out underex situconditions and subsequently placed into a rigid vacuum typically in the range of less than 3.5×10^{-7} Pa. The adventitious peak of carbon at 284.6 eV was considered as the internal reference. The chemical state was evaluated through the peaks areas from the curve fitting of the regions of Pt 4f and Pd 3d employing the XPSPEAK computer program.

1.5 Density Functional Theory (DFT) calculations

Calculate methods: All DFT calculations were performed using the VASP program.[1, 2] The DFT functional was utilized at the Perdew−Burke−Ernzerhof (PBE) level.[3] The project-augmented wave (PAW) method was used to represent the core−valence electron interaction. A 2×2×1 gamma grid of k-points was used for the Brillouin zone integration. The valence electronic states were expanded in plane-wave basis sets with an energy cutoff at 520 eV. Gaussian smearing of 0.05 eV was applied during the geometry optimization. The convergence criteria for the iteration in the self-consistent field (SCF) were set at 10-5 eV, and the residual force for optimizing atom positions was less than 0.02 eV/Å.

1.6 Products analysis

The process of product analysis was introduced with glucose dehydrogenation reaction as an example, and the same method was used in other experiments. The reaction product is acidified with aqueous H_2SO_4 0.01 M(acidification of gluconate to gluconic acid). Analyses were performed on a liquid chromatograph (Waters 1500, USA) equipped with a Waters 2998 PDA (the absorbed wavelength was 210 nm) and

a Waters 2414 R.I. detectors. A Hi-Plex H column (7.7 mm × 300 mm × 8 μm) was used with aqueous H_2SO_4 0.01M (0.6 mL/min) as the eluent.

The MS(Q Exactive Plus) condition was summarized as follows: 3000 V for capillary voltage, 300 °C for capillary temperature, 250 °C for vaporizer temperature, 35 for sheath gas pressure, and 10 for aux gas pressure. Nitrogen was used for the sheath and auxiliary gas.

NMR spectra of products were detected by Bruker Avance III 500 spectrometer.

The conversions of D-glucose, and the yields of products, such as hexitol, potassium formate and potassium gluconate, were calculated as follows：

Conversion (%) =

$$\left\{1-\frac{molar\ concentration\ of\ glucose\ remained}{molar\ concentration\ of\ glucose\ introduced}\right\}\times 100\%$$

yield of hexitol (%) =

$$\left\{\frac{molar\ concentration\ of\ hexitol\ produced}{molar\ concentration\ of\ glucose\ introduced}\right\}\times 100\%$$

yield of gluconic acid (GNA) =yield of potassium gluconate (%) =

$$\left\{\frac{molar\ concentration\ of\ potassium\ gluconate\ produced}{molar\ concentration\ of\ glucose\ introduced}\right\}\times 100\%$$

yield of formate (%) =

$$\left\{\frac{molar\ concentration\ of\ potassium\ formate\ produced}{molar\ concentration\ of\ potassium\ carbonate\ introduced}\right\}\times 100\%$$

2 Supporting Tables

Table S1 Effect of solvent composition on the simultaneous transformation of glucose and K_2CO_3.

Solvent	Glucose Conv. (%)	Formate Yield (%)	GNA Yield (%)
H_2O	51.2	5.3	48.8
50 % MeOH	65.9	10.9	55.5
50 % EtOH	69.7	47.4	60.3
50 % 1-PrOH	67.5	32.2	56.6
10 % EtOH	49.8	8.7	39.7
25 % EtOH	56.2	24.0	45.3
75 % EtOH*	-	-	-

Reaction conditions: 30 °C; 20 h; catalyst: 0.1 g; 0.06 mol mL^{-1} glucose solution (20 mL ethanol + 20 mL H_2O); 0.16 g K_2CO_3

* The solubilites of glucose and carbonate were very low in the 75 wt% ethanol solution.

To investigate the effect of alcohols, further reactions were performed using x vol% (x = 0, 10, 25, 50, 75) alcohol in water as the solvent. Our previous work showed that increasing the proportion of alcohols can promote the dehydrogenation of glucose. The degree of substrate hydration also affects catalytic activity because water molecules around the substrate can interfere with substrate adsorption on the metal surface. Alcohols are known to disrupt the hydrogen-bonded structure of water,[4] which facilitates the adsorption of reactants on the metal surface. Nevertheless, excess alcohol leads to carbonate precipitation. Therefore, 50 vol% was selected. In a previous study, the use of ammonium salts and an ethanol-water solution enhanced the formic acid yield, which was attributed to the formation of ethyl carbonate. To confirm this possibility, K_2CO_3 alcoholic solutions were prepared and analysed using 13C NMR spectroscopy (Fig. S10). The K_2CO_3 solutions only exhibited carbonate and solvent peaks. This indicated that alkyl carbonate was not the intermediate species in our system and that the increased formic acid yields in the alcoholic solutions were due to other factors. The higher H_2 solubility and enhanced dispersion of carbon-based catalysts in alcoholic solutions compared with their dispersion in water are likely responsible for the enhanced product yields.[5,6]

Table S2. The effect of CO_2 source on the transfer hydrogenation of carbonates.

CO_2 source	pH	Glucose Conv. (%)	Yield (%)		
			GNA	Formate	Alditol
Na_2CO_3	11.0	64.4	55.5	33.6	7.6
K_2CO_3	11.2	69.7	60.3	47.4	9.1
Rb_2CO_3	11.2	71.1	61.9	48.9	8.3
Cs_2CO_3	11.3	72.8	63.1	51.0	8.5

Reaction conditions: 30 °C; 20 h; catalyst: 0.1 g; 0.06 mol mL^{-1} glucose solution (20 mL ethanol + 20 mL H_2O); 0.07mol/L g carbonate

Table S3 XPS surface element analysis of Pt_xPd_y/CNTs.

Catalysts	Surface metal atomic content		
	Pt	Pd	Pt/Pd
Pt_4Pd_1/CNTs	0.22	0.13	1.69
Pt_3Pd_2/CNTs	0.14	0.17	0.82
$Pt_1Pd_{1.2}$/CNTs	0.11	0.26	0.42
Pt_2Pd_3/CNTs	0.08	0.34	0.24
Pt_1Pd_4/CNTs	0.06	0.49	0.12
Pt_2Pd_3/CNTs-used	0.09	0.33	0.27

3 Supporting Figures

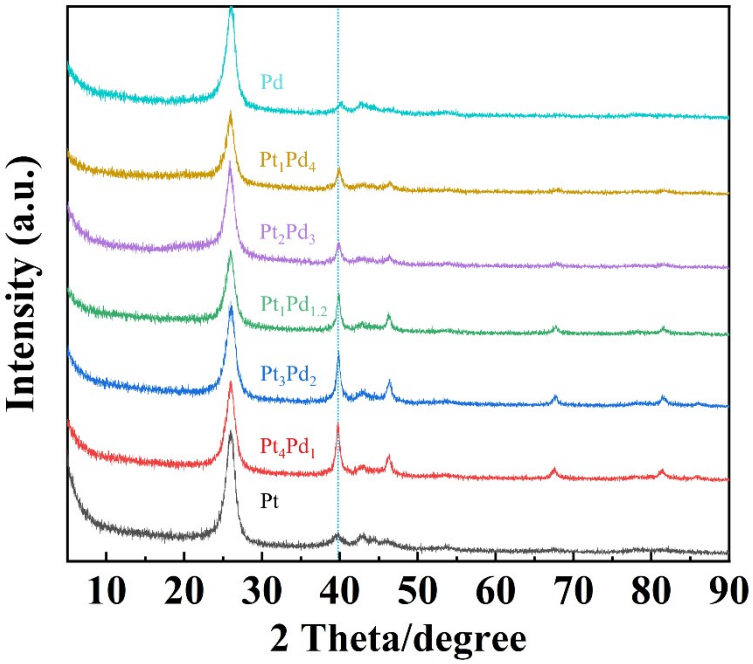

Fig. S1 XRD patterns of Pt_xPd_y/CNTs.

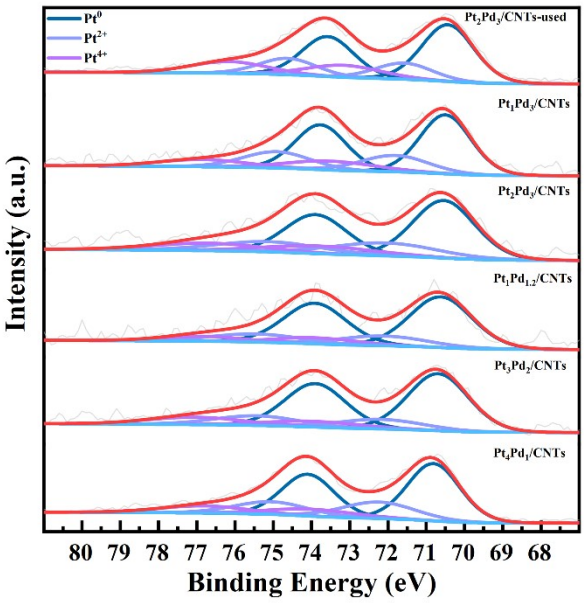

Fig. S2 Pt 4f XPS spectra of Pt_xPd_y/CNTs alloy catalysts.

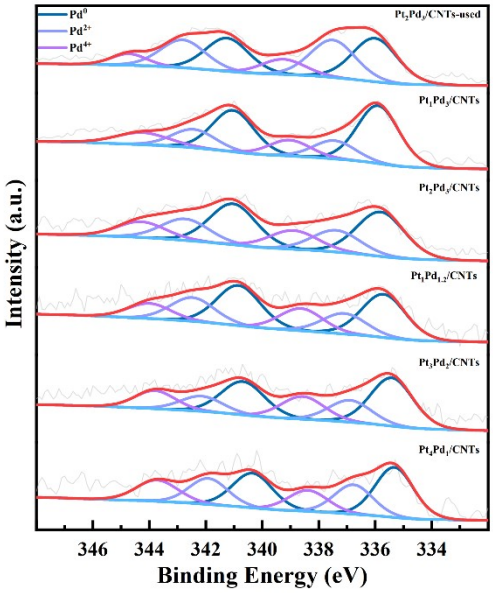

Fig. S3 Pd 3d XPS spectra of $Pt_xPd/_yCNTs$ alloy catalysts.

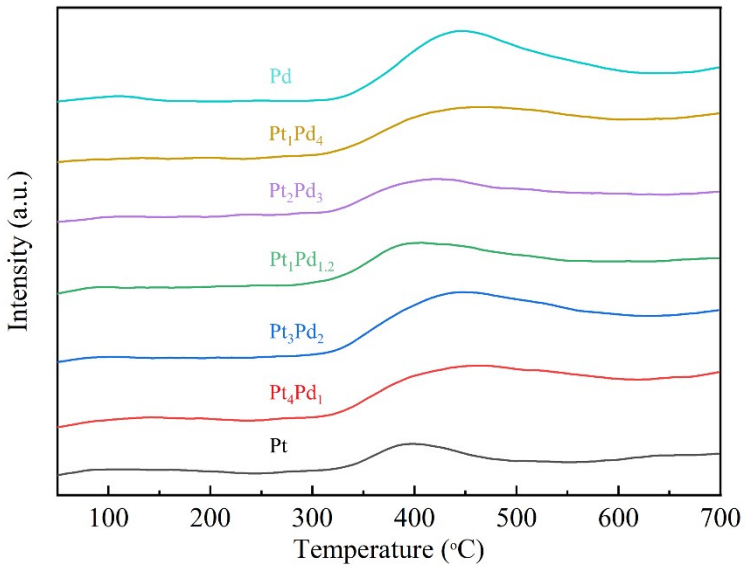

Fig. S4 H_2-TPD of Pt_xPd_y/CNTs.

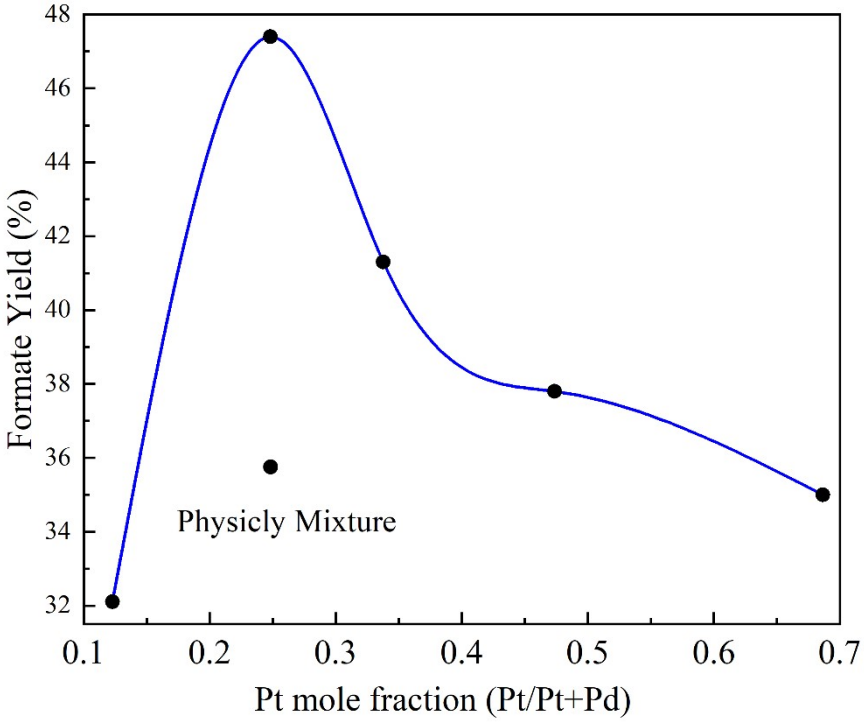

Fig. S5 Yield of formate versus Pt mole fraction.

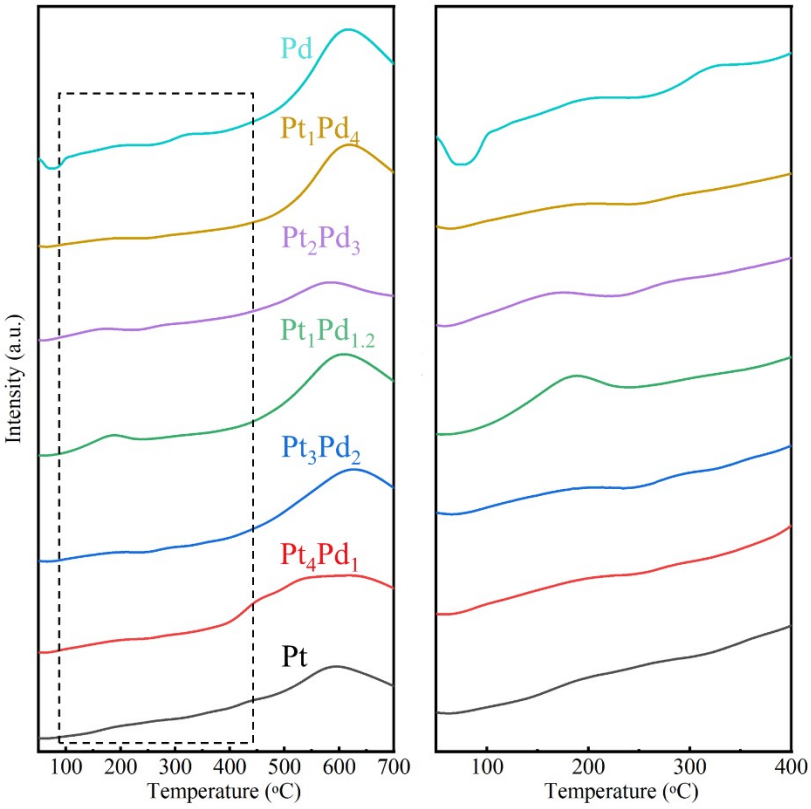

Fig. S6 H_2-TPR of Pt_xPd_y/CNTs.

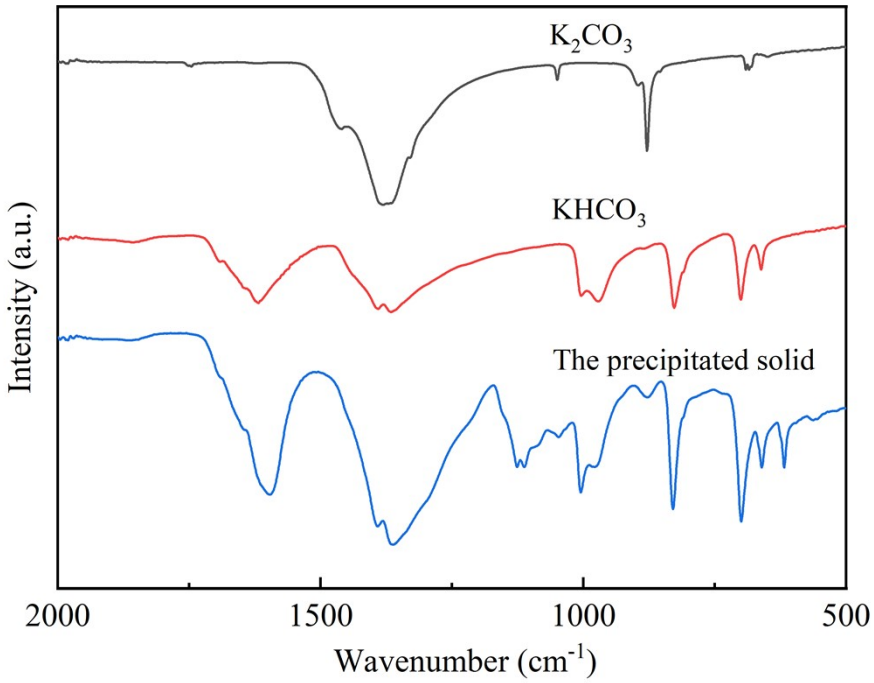

Fig. S7 ATR-FTIR spectra of the K_2CO_3, $KHCO_3$ and the precipitated solid.

The reaction product was filtered to separate the solid catalyst. Addition of excessive ethanol led to crystal precipitation, at which point K_2CO_3 or $KHCO_3$ precipitated (K_2CO_3 and $KHCO_3$ would precipitate in higher concentration of ethanol-water mixed solvent) and was removed by filtration，the crude was analysed by ATR-FTIR(impurity is potassium gluconate).

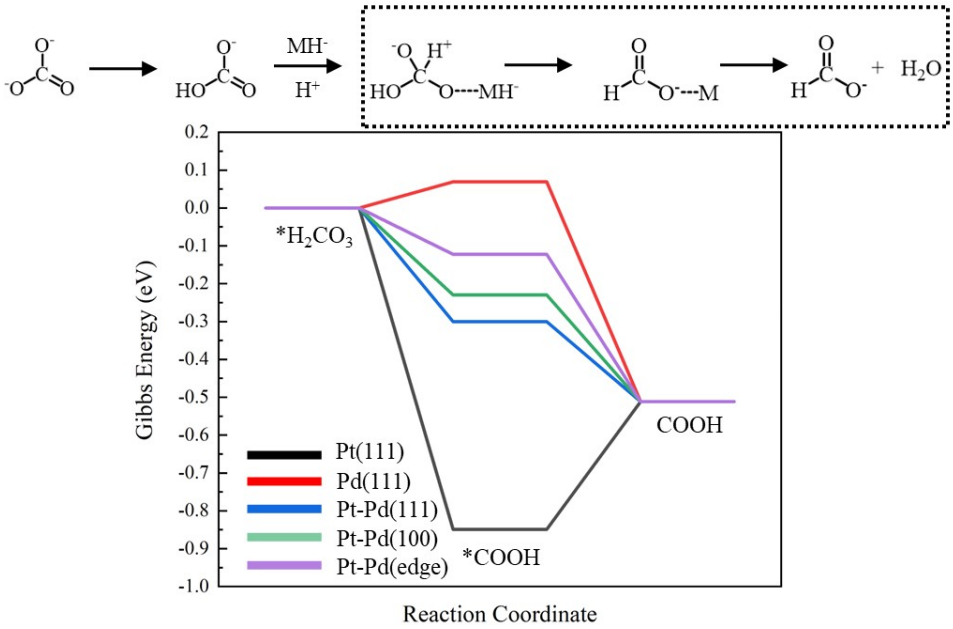

Fig. S8 The DFT calculation results: the reaction energy diagram for the desorption of formate on Pt(111), Pd(111), Pt-Pd(111), Pt-Pd(100) and Pt-Pd(edge).

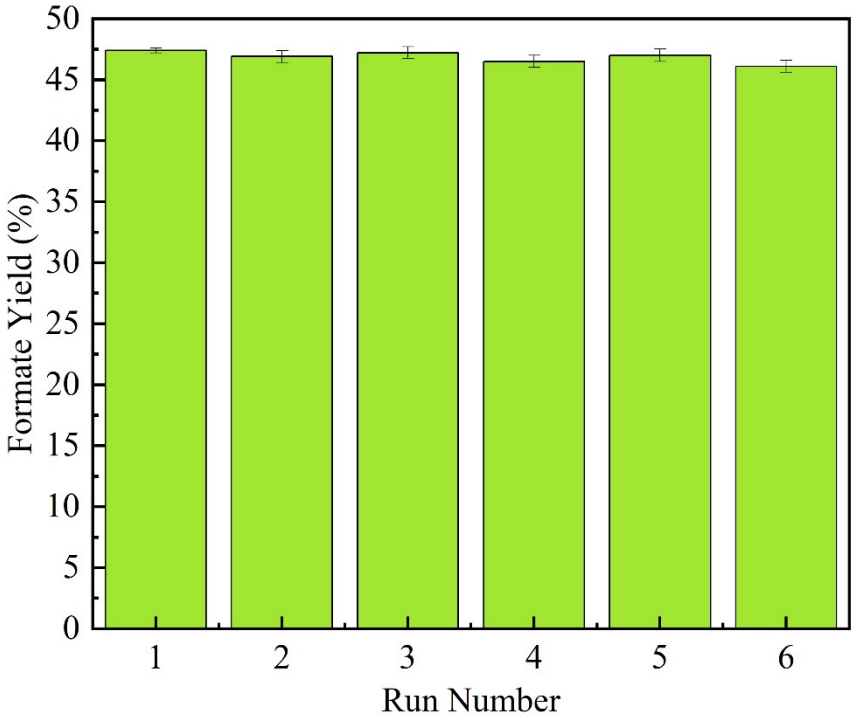

Fig. S9 Catalyst recycling.

Reaction conditions: 30 °C; 20 h; catalyst: 0.1 g; 0.06 mol mL^{-1} glucose solution (20 mL ethanol + 20 mL H_2O); 0.16 g K_2CO_3

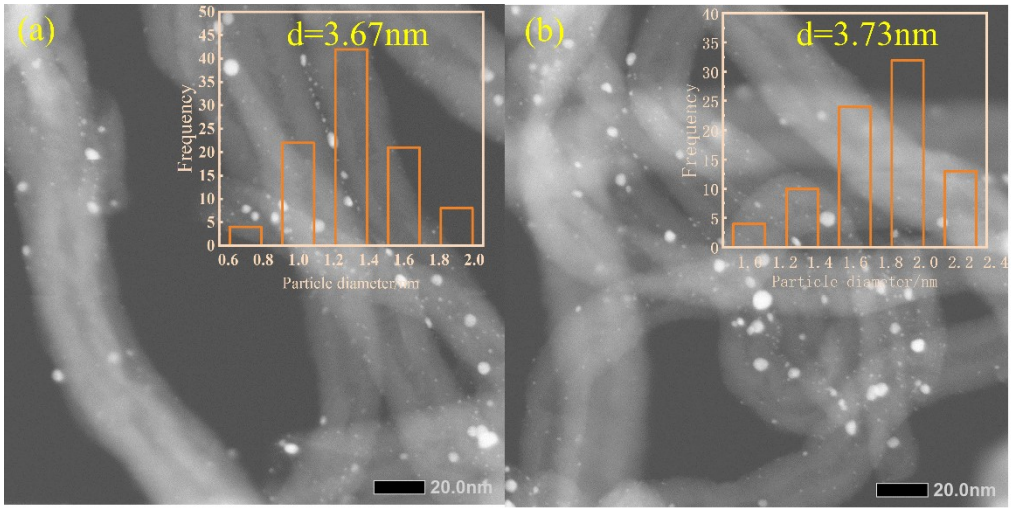

Fig. S10 Particle size distributions and TEM images of Pt_2Pd_3/CNTs: (a) Pt_2Pd_3/CNTs. (b) Pt_2Pd_3/CNTs-used.

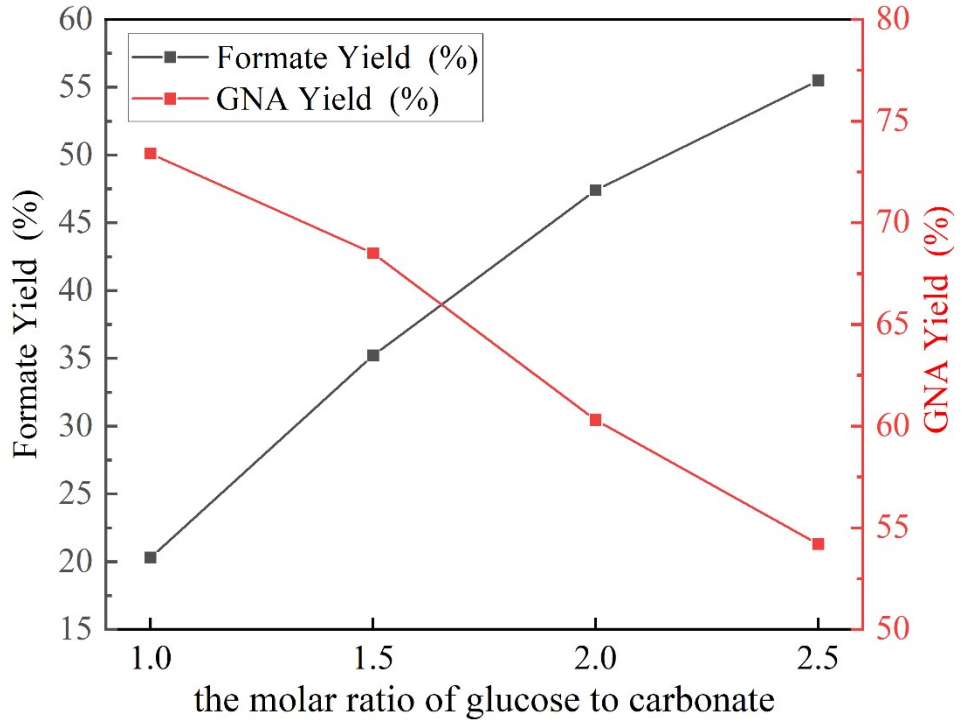

Fig. S11 Effect of the amount of glucose when the amounts of potassium carbonate is fixed. Reaction conditions: 30 °C; 20 h; catalyst: 0.1 g; x(x=0.03, 0.045, 0.06, 0.075) mol mL^{-1} glucose solution (20 mL ethanol + 20 mL H_2O); 0.16 g K_2CO_3

Although the stoichiometric ratio of glucose and potassium carbonate was 1:1, the yield of formic acid was not high at this ratio. Increasing the amount of glucose, the hydrogen donor, improved the yield of formic acid, although excess glucose led to its wastage. The market price of glucose is $280/ton and that of gluconate is $500/ton.[7] When the yield of gluconate reaches 56%, the semi-reaction of glucose dehydrogenation is profitable, i.e., glucose will not be wasted. Therefore, the optimum molar ratio of glucose to carbonate is 2:1. It is common for the amount of hydrogen donor to be slightly higher than the stoichiometric ratio in the hydrogen conversion reaction. For example, in the transfer hydrogenation of various unsaturated aldehydes and ketones using glucose as the hydrogen source, as reported by Fujita et al.[8], the molar ratio of glucose to ketones or aldehydes was 2: 1. An appropriate feed ratio should be selected considering the economic value of the substrate and product.

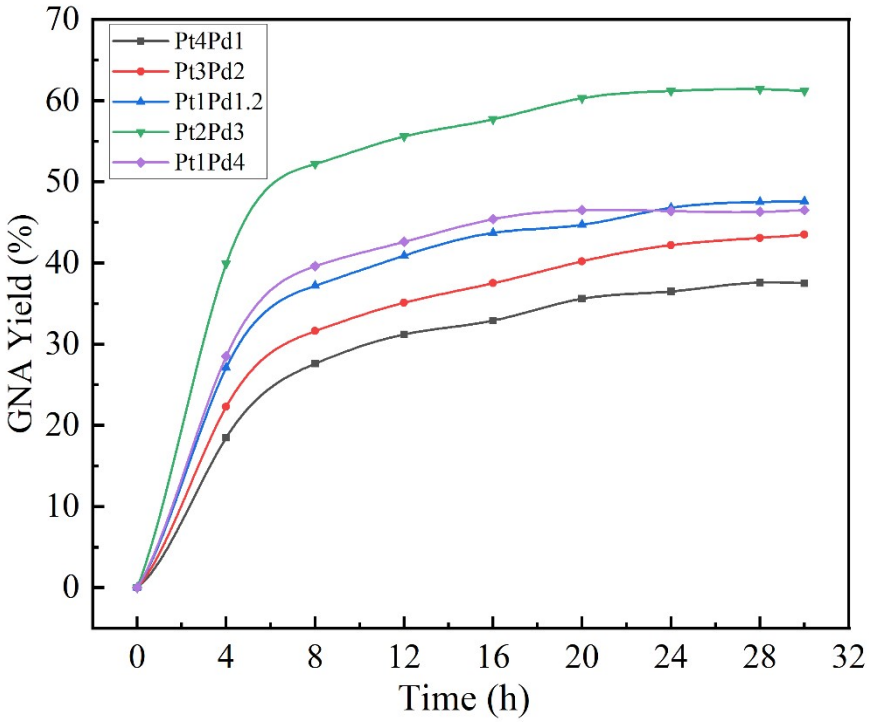

Fig. S12 GNA yield versus reaction time.

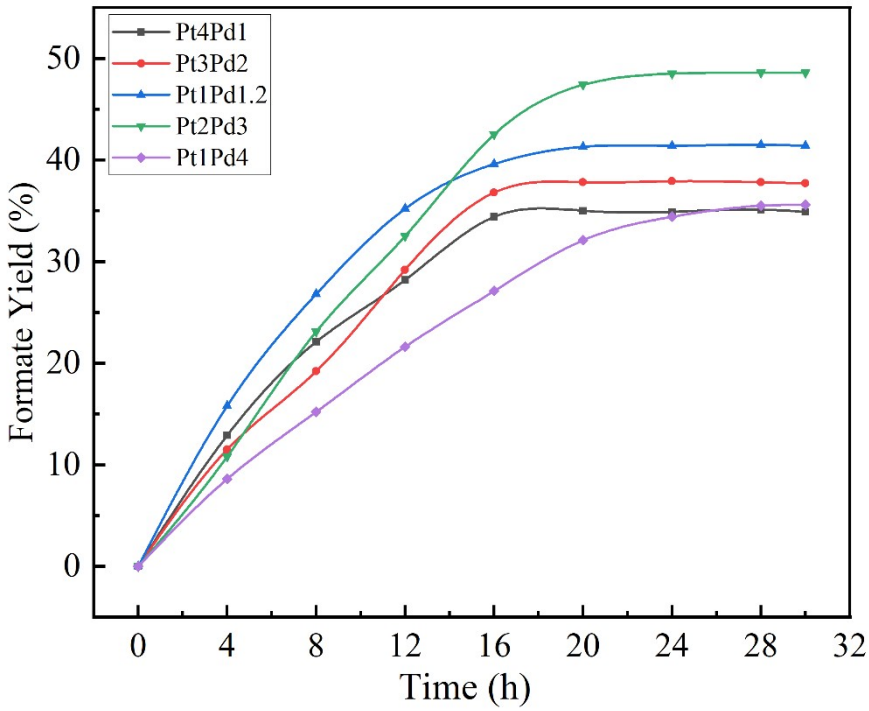

Fig. S13 Formate yield versus reaction time.

The transient yields of GNA and formate show that carbonate hydrogenation is more difficult than glucose dehydrogenation, which is consistent with the results of the theoretical calculations.

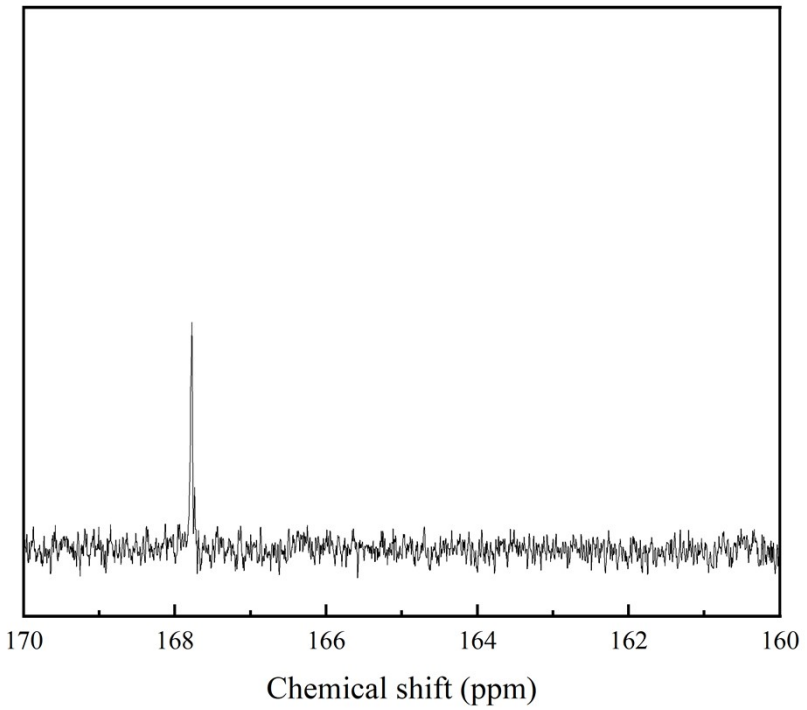

Fig. S14 The ^{13}C NMR spectra of 0.16g K_2CO_3 in 50% alcohol/D_2O solutions.

References

[1] Furthmüller, J. and G. Kresse, Efficient iterative schemes for ab initio total-energy calculations using a plane-wave basis set. *Phys. Rev. B*, **1996**. 54, 11169-11186.
[2] Kresse, G. and J. Furthmüller, Efficiency of ab-initio total energy calculations for metals and semiconductors using a plane-wave basis set. *Copm. Mater. Sci.* **1996**, 15-50.
[3] Burke, K., M. Ernzerhof and J.P. Perdew, Generalized Gradient Approximation Made Simple. *Phys. Rev. Lett*, 1996, 3865-3868.
[4] V. Matvejev, M. Zizi and J. Stiens, *J. Phys. Chem. B*, **2012**, 116, 14071-14077.
[5] M. S. Wainwright, T. Ahn, D. L. Trimm and N. W. Cant, *J. Chem. Eng. Data*, 1987, **32**, 22-24.
[6] J. V. H. d 'Angelo and A. Z. Francesconi, *J. Chem. Eng. Data*, 2001, **46**, 671-674.
[7] http://www.alibaba.com/?spm=a2700.7699653.a271qf.40.APWJep
[8] M. Yoshida, R. Hirahata, T. Inoue, T. Shimbayashi, K. Fujita, *Catalysts* **2019**, *9*. 503-515.